

Article

Research on Path Planning in 3D Complex Environments Based on Improved Ant Colony Algorithm

Hang Zhou, Ziqi Jiang *, Yuting Xue, Weicong Li , Fanger Cai and Yunchen Li

College of Civil Aviation, Nanjing University of Aeronautics and Astronautics, Nanjing 211100, China

* Correspondence: allezq@nuaa.edu.cn; Tel.: +86-156-6360-9207

Abstract: Aiming at the problems of complex space, long planning time, and insufficient path security of 3D path planning, an improved ant colony algorithm (TGACO) is proposed, which can be used to solve symmetric and asymmetric path planning problems. Firstly, the 3D array is used to access the environment information, which can record the flight environment and avoid the inefficiency of planning. Secondly, a multi-objective function of distance and angle is established to improve the efficiency and safety of the path. Then, a target-guided heuristic function is proposed, and an anti-deadlock mechanism is introduced to improve the efficiency of the ant colony algorithm. Next, the node pheromone update rules are improved to further improve the efficiency of the algorithm. Finally, experiments prove the effectiveness of the improved algorithm, TGACO, and its efficiency in complex environments has obvious advantages. In the $20 \times 20 \times 20$ environment, compared with the ant colony algorithm (ACO), the improved algorithm (TGACO) in this paper improves the path length, total turning angle, and running time by 17.8%, 78.4%, and 95.3%, respectively.

Keywords: target guidance; anti-deadlock; path angle; node pheromone; ACO



Citation: Zhou, H.; Jiang, Z.; Xue, Y.; Li, W.; Cai, F.; Li, Y. Research on Path Planning in 3D Complex Environments Based on Improved Ant Colony Algorithm. *Symmetry* **2022**, *14*, 1917. <https://doi.org/10.3390/sym14091917>

Academic Editor: Axel Pelster

Received: 22 July 2022

Accepted: 15 August 2022

Published: 13 September 2022

Publisher's Note: MDPI stays neutral with regard to jurisdictional claims in published maps and institutional affiliations.



Copyright: © 2022 by the authors. Licensee MDPI, Basel, Switzerland. This article is an open access article distributed under the terms and conditions of the Creative Commons Attribution (CC BY) license (<https://creativecommons.org/licenses/by/4.0/>).

1. Introduction

In recent years, military and civilian UAV technology has developed rapidly. UAVs are used in agriculture and forestry, electric power, logistics and target attack, etc. However, no matter what kind of scenarios and tasks a UAV is applied in, flight path planning is indispensable. UAV path planning is a planned route that connects from the starting point to the target point and avoids obstacles according to mission requirements, flight environment, and other information. Path planning is an NP-hard problem. Unlike path planning of mobile robots, path planning involves three-dimensional space, so the planning space is more complicated and the calculation amount is larger, which requires a higher calculation speed of the algorithm. Due to the constraints of the UAV itself, the safety requirements of the flight path are stricter. Combined with the constraints, the quality requirements of flight modeling and flight path solution of the UAV are more demanding.

At present, UAV path planning is mostly solved by intelligent optimization algorithms [1–3], mainly focusing on the path symmetry planning problem. That is, the equal round-trip cost between two path points is a symmetry problem, and the unequal cost is an asymmetric problem. Paper [4] proposed an improved artificial potential field method, which introduced angle and speed adjustment factors and set auxiliary obstacle avoidance forces at the same time to ensure the safe and smooth path and conform to the real path of UAVs. Paper [5] uses the Metropolis criterion and RTS smoothing algorithm to improve the PSO algorithm, solve the problem that the algorithm is easy to fall into local optimization, further smooth the path, and optimize the path planning results. Paper [6] designed the coding method according to the characteristics of the 3D path, then adjusted the crossover and mutation operators and designed the dynamically adjusted nonlinear fitness function, which improved and solved the premature problem of the genetic algorithm and improved the convergence speed, but the disadvantage is that there are infeasible paths that need to

be judged again. Paper [7] introduced an adaptive adjustment factor to improve the ant colony algorithm to balance convergence and global search capabilities, and improved high-quality node selection probability with the angle guidance factor and obstacle elimination factor, so that path planning has high real-time use and stability. Paper [8] improved PRM to transform the flight environment into an undirected connected graph while increasing the number of samples near obstacles to improve the quality of the shortest path of the ant colony algorithm in complex terrain, but the path completely depends on the number and location of sampling points, and the feasible path is not complete. Paper [9] proposed a layered ant colony algorithm for 3D path planning, which takes the combination of an obstacle, distance, and height as the heuristic function and uses the way of track point projection to reduce the dimension of 3D space and improve the efficiency of the algorithm. Paper [10] designed an environment space coordinate transformation method, which adopts adaptive pheromone update and uses distance and angle between the next node, the current point, and the target point as inspiration to improve the global search ability and efficiency of the ant colony algorithm, but the calculation method of the algorithm is complex, and the amount of calculation is large.

To sum up, the space search of UAV 3D path planning is complex, and dimension reduction is adopted in some studies, which results in some possible paths being ignored. Moreover, some 3D planning coding methods are complicated, and there are infeasible paths that need to be judged again. Then, the guidance of target points to the path is less considered in path planning, and the calculation is large and complex, resulting in the insufficient calculation accuracy and low time efficiency. Therefore, this paper proposes an improved ant colony algorithm for fast path planning, and the main work involved is as follows: (1) a 3D array flight environment model is established, and the storage of environmental information directly corresponds to the dimensions, which reduces the complexity of space conversion, improves the efficiency of information reading, and makes flight path planning more consistent with the actual flight environment. (2) The multi-objective function of path planning combining total distance and total angle is established to reduce the number of turns and angles and improve the safety of path planning while obtaining the shortest path. (3) Cross-grid path search is prohibited to avoid the occurrence of an infeasible path, so there is no need to judge the feasibility of the path. (4) In the algorithm, the target guidance mechanism and anti-deadlock mechanism are designed to improve the target guidance of the search, and then the invalid nodes are marked to improve the efficiency of the algorithm and the quality of the path solution. The node pheromone updating method is adopted to reduce the corresponding relationships between nodes and edges to improve the computational efficiency of the ant colony algorithm. (5) Simulation results show that the improved algorithm is efficient and correct. The detailed structure of this paper is: (1) research background, (2) UAV flight model establishment, (3) algorithm design, (4) simulation and analysis, and (5) conclusion.

2. Model Establishment

2.1. Flight Environment Model

Flight environment construction is the basis of UAV flight path planning. This paper establishes a 3D environment model for the UAV flight. Compared with a 2D plane, 3D modeling can more truly reflect the UAV flight environment. As shown in Figure 1, the space rectangular coordinate system of x , y , and z axes is established, and the flight environment is divided by the grid method. The grid method is a common method in path planning. It refers to dividing the flight space into a certain number of grids [11], and each grid represents a searchable space. The size of the unit grid directly affects the accuracy and complexity of UAV path planning. The division of the unit grid is too large and the accuracy of the UAV path is insufficient, which affects the final path distance and cannot ensure a better-planned path. The unit grid division is too small and the complexity of path planning is high, which increases the time required for path planning. Therefore, this paper selects the minimum path segment of UAV as the basis of grid division, which can not only

ensure the path accuracy of UAV but also meet the design requirements of a UAV. Then, by marking the known environmental information, 0-obstacle, 1-flight, and using a 3D array to store the flight environment information converted into digital markers, we are able to facilitate the subsequent intelligent algorithm to read the flight environment and then plan the flight path of the UAV. At the same time, using a 3D array to record information can avoid the conversion of spatial dimensions and improve the computational efficiency of the algorithm.

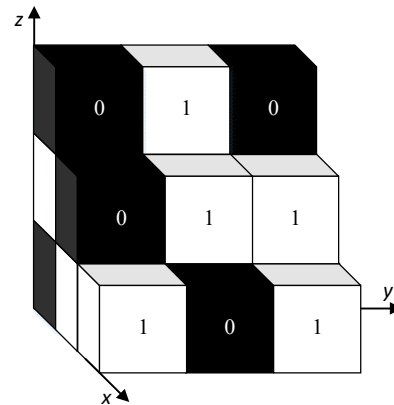


Figure 1. The 3D flight environment model.

2.2. Path Planning Model

2.2.1. Objective Function

The establishment of an objective function directly affects the evaluation of the path. To ensure that the planned UAV has the shortest path distance and the least turning times, a multi-objective function composed of the total path distance and the total turning angle is established in this paper. The establishment of a multi-objective function is used to solve the problem of insufficient path safety of UAVs, while ensuring the shortest flight distance of UAVs, reducing the number and degree of changing flight attitude, and balancing the relationship between flight distance and attitude change to improve the flight safety of UAVs. The objective function is shown in Equation (1).

$$f(x) = \lambda_1 \sum_{i=1}^n l_i + \lambda_2 \sum_{j=1}^{n-1} \theta_j \quad (1)$$

where l_i is the distance of the path segment, θ_j is the included angle between the path segments, and λ_1 and λ_2 are the weights of the total distance and angle, respectively.

2.2.2. Constraints

Due to the design requirements of the UAV, the planned path needs to meet the physical characteristics of the UAV. In this paper, the maximum turning angle, the maximum pitching angle, and the maximum path distance are selected as the UAV path constraint conditions [12].

(1) Maximum turning angle: the maximum angle allowed by the UAV in a turn during flight. The maximum turning angle can be calculated by the included angle between two paths. As shown in Figure 2, α is the angle of a turn of a UAV, which is calculated as shown in Equation (2).

$$\frac{a_i \cdot a_{i+1}^T}{|a_i| \times |a_{i+1}|} \geq \cos \alpha \quad (i = 1, 2, \dots, n-1) \quad (2)$$

where a_i is the path segment vector, and $|a_i|$ is the length of the path segment vector.

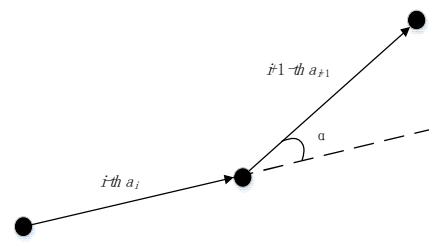


Figure 2. Schematic diagram of the maximum turning angle.

(2) Maximum pitch angle: the maximum angle allowed to change when the UAV rises or dives in the vertical direction. As shown in Figure 3, the included angle between the path segment and its projection on the horizontal plane ζ is the rising or diving angle, and the angle calculation is shown in Equation (3).

$$\frac{|b_i|}{|a_i|} \leq \tan \zeta \quad (i = 1, 2, \dots, n) \quad (3)$$

where $|b_i|$ is the difference in the vertical direction of the path segment, and $|a_i|$ is the length of the path segment vector.

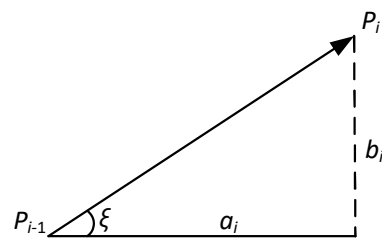


Figure 3. Schematic diagram of maximum pitch angle.

(3) Maximum path distance: the maximum distance that the UAV can fly at a constant speed in a mission. The constraint condition is shown in Equation (4).

$$\sum_i l_i \leq L_{\max} \quad (i = 1, 2, \dots, n) \quad (4)$$

where l_i is the distance of the path of segment i , and L_{\max} is the preset maximum path distance.

3. Improved Ant Colony Algorithm

UAV path planning is a route that connects from the starting point to the ending point and bypasses obstacles according to mission requirements, flight environment, and other information. At the same time, the flight path should meet the constraints of the UAV to ensure flight safety. After analyzing the commonly used algorithms for UAV flight path planning [13–15] and the structure of the flight path solution, this paper selects the ant colony algorithm to solve the 3D flight path of UAV. The ant colony algorithm has good parallelism, cooperation, and robustness, and the greedy mechanism drives the solution to the optimal. Moreover, the ant colony algorithm has no crossover mutation or other operations, resulting in the chaos of the path solution order. It has no specific requirements for the symmetry of the graph and objective function, and can solve symmetric, asymmetric, linear, and nonlinear problems, so it is more suitable for UAV path planning.

3.1. Ant Colony Algorithm

As a heuristic intelligent algorithm for solving optimization problems, the ant colony algorithm is also commonly used in path planning [16–21]. The basic idea is to use the positive feedback mechanism to leave pheromones along the path of ants, and the better the path is, the more pheromones are generated. The selection probability of ants is calculated

according to the pheromone and heuristic function, and then the optimal solution is found through continuous iteration. The calculation equations of the traditional ant colony algorithm are shown in Equations (5)–(7), which are heuristic function, state transition probability, and pheromone update, respectively.

$$\eta_{ij}(t) = \frac{1}{d_{ij}} \quad (5)$$

$$p_{ij}^k(t) = \begin{cases} \frac{\tau_{ij}^\alpha(t) \times \eta_{ij}^\beta(t)}{\sum_{s \in J_k(i)} \tau_{ij}^\alpha(t) \times \eta_{ij}^\beta(t)} & j \in J_k(i) \\ 0 & \text{Otherwise} \end{cases} \quad (6)$$

$$\begin{aligned} \tau_{ij}(t+1) &= \tau_{ij}(t) \times (1 - \rho) + \Delta\tau_{ij} \\ \Delta\tau_{ij} &= \sum_{k=1}^m \Delta\tau_{ij}^k \\ \Delta\tau_{ij}^k &= \begin{cases} \frac{Q}{L_k} & k \text{ ant passes by } ij \\ 0 & \text{Otherwise} \end{cases} \end{aligned} \quad (7)$$

where τ_{ij} is pheromone, η_{ij} is the heuristic function, d_{ij} is the distance from grid i to grid j , α is the pheromone factor, β is the heuristic function factor, ρ is the pheromone volatilization coefficient, Q is the pheromone constant, L_k is the path length of this iteration, and $\Delta\tau_{ij}$ is the pheromone increment of this iteration.

3.2. Improvement Heuristic Function

The heuristic function of the ant colony algorithm is guided by the distance between the current point and the selected node, while the orientation of the target point is not considered. As the end node of the whole path, the position relationship between the target point, the current point, and the selected node are particularly important. The closer the selection node is, the better the connection between the current point and the target point is. That is, the more the vector between the current point and the selection node points to the target point, the greater the probability that the selected node should be selected. Usually, there are 26 selectable nodes near a node, and the guidance of the target point to these selectable nodes is different. If the difference between the advantages and disadvantages of nodes can be distinguished effectively, the ant can preferentially select nodes with better quality, thus improving the efficiency of the algorithm. Therefore, the improved heuristic function of the target guidance mechanism is proposed in this paper, as shown in Equations (8) and (9). The known information of the UAV flight environment is fully utilized, enhancing the influence of the target point on the whole path, making it easier for the ant colony to find the path segment pointing to the target point, thus effectively improving the convergence speed of the algorithm. According to the target guidance mechanism, Equation (9), C^G-S^G is in the range of $[-3,3]$ and T^G is in the range of $[0,1]$. The larger the value, the smaller the angle between the vector from the current point to the selected point and the vector from the current point to the target point, and the better the target directivity. As shown in Figure 4, the target guidance values of the 26 nodes around the current point have symmetry, wherein the target guidance value of the S1 node on the vector line segment from the current point to the target point is 1, the target guidance value of the other nodes decreases gradually, and the target guidance value of the node away from the vector line segment is 0. Therefore, the selection point S1 pointing to the target point is more enlightening.

$$\eta_j(t) = \mu_1 \frac{1}{d_{ij}} + \mu_2 T^G \quad (8)$$

where d_{ij} is the distance between the current grid i and the selected grid j , T^G is the normalization of the target point guidance value in the interval $[0,1]$, and μ_1 and μ_2 represent the corresponding weight, respectively. When $\mu_1 = 1$ and $\mu_2 = 0$, the heuristic

function is the distance heuristic of the traditional ant colony algorithm. When $\mu_1 = 0$ and $\mu_2 = 1$, the heuristic function is target-guided heuristic. The larger μ is, the stronger the corresponding distance or target guidance enlightenment is.

$$\begin{aligned} T^G &= (\sin((C^G - S^G) \times \frac{\pi}{6}) + 1)/2 \\ C^G &= |t_x - c_x| + |t_y - c_y| + |t_z - c_z| \\ S^G &= |t_x - s_x| + |t_y - s_y| + |t_z - s_z| \end{aligned} \quad (9)$$

where C^G is the guidance of the target point to the current point, S^G is the guidance of the target point to the selected node, t_x , c_x , and s_x are the grid x-axis indexes of the target point, the current point, and the selected node, respectively, t_y , c_y , and s_y are the grid y-axis indexes of the target point, the current point, and the selection node, respectively, and t_z , c_z , and s_z are the grid z-axis indexes of the target point, the current point, and the selection node, respectively.

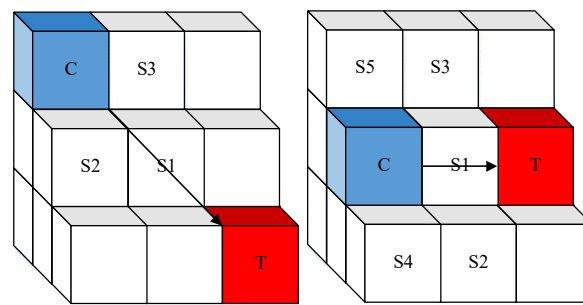


Figure 4. Schematic diagram of target guidance mechanism.

3.3. Anti-Deadlock Path

Due to the influence of the flight environment, the ant colony may fall into the surrounding obstacles when looking for the path node. As shown in Figure 5, there are no selectable nodes around the current point, and the ant colony algorithm falls into a deadlock, thus failing to find the track from the starting point to the target point. Therefore, this paper designs a mechanism to jump out of obstacles to prevent algorithm deadlock. If there is no selectable node around the current point, jump out of the current point, return to the previous node, and mark the current point to prevent entering the enclosure again. Release the marking information until the next feasible path node is successfully selected. This mechanism can ensure that the ant colony algorithm can obtain an effective path from the starting point to the target point, reduce the possibility of obtaining invalid paths, and improve the quality of each ant colony's search solution.

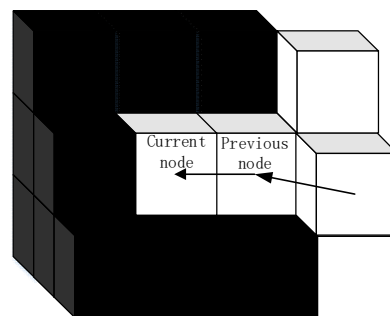


Figure 5. Schematic diagram of anti-deadlock mechanism.

3.4. Improvement Pheromone Update

In the development of the ant colony algorithm, two main pheromone storage structures have been developed: edge pheromone and node pheromone [22]. Most ant colony algorithms use edge pheromones to update and store, which is related to the structure of the

path planning solution. Due to the complexity of spatial search and numerous node-edge paths in the 3D path planning of UAV, the storage space of the edge pheromone structure is huge, and the corresponding relationship of nodes is complex, which is not conducive to the algorithm's solution. In addition, this paper establishes a 3D array model for UAV flight environment information, which is more convenient for the use of node pheromone structure, reduces the mapping relationship between nodes, and further improves the efficiency of the algorithm. Through the above improvements, the space complexity of this paper is the space complexity $O(n^3)$ of the 3D array. In the ant colony algorithm using the node pheromone, there is a problem that a node may pass through multiple association paths. Each association path will generate a pheromone and update at the node, which makes the pheromone distribution of the node increase sharply [23]. To avoid the rapid accumulation of node pheromones, the strategy of global pheromone update should be adopted. When the global pheromone update strategy is adopted, it can appropriately slow down the trend of rapid accumulation of node pheromones, but there is still instability. Therefore, this paper considers that only the pheromone of the optimal solution is updated in the early stage of the algorithm iteration to reduce the updating of the pheromone of inferior nodes, and the pheromone of each solved path is updated in the middle and late stage of the algorithm iteration. When each time is $t + 1$, the pheromone update is shown in Equations (10) and (11).

$$\tau_j(t+1) = \tau_j(t) \times (1 - \rho) + \Delta\tau_j \quad (10)$$

$$\Delta\tau_j^k = \begin{cases} \frac{Q}{L_{best}} & \begin{matrix} \text{The early of iteration,} \\ k \text{ ant passes through node } j \end{matrix} \\ \frac{Q}{L_k} & \begin{matrix} \text{The middle and later of the iteration,} \\ k \text{ ant passes through node } j \end{matrix} \\ 0 & \text{Otherwise} \end{cases} \quad (11)$$

where ρ is the pheromone volatilization factor, Q is the pheromone constant, L_{best} is the current optimal path length, and L_k is the path length found by ant k .

3.5. Improvement Algorithm Flow

To avoid the planned path crossing obstacles and carrying out collision tests later, a cross-grid search by ants is forbidden in this paper. Therefore, the selectable nodes searched by ants each time are the adjacent grid of the current point. At the same time, the grid that does not meet the maximum turning angle and maximum pitch angle is deleted to avoid invalid searches by ants and improve the search efficiency of the ant colony algorithm. The specific algorithm implementation steps are as follows:

- (1) Input the starting point, target point, minimum direct flight distance, and other parameters, build the flight environment grid map, and create a 3D array of environment information.
- (2) Initialize the algorithm parameters, and set the maximum number of iterations of the ant colony algorithm, the number of ants, heuristic function factor, pheromone factor, volatilization coefficient, etc.
- (3) Path selection: the ant calculates the state transition probability according to the target guidance mechanism, selects the next path node, and avoids generating invalid paths according to the anti-deadlock mechanism until the target point is found.
- (4) Pheromone updating: according to the pheromone updating rules, the pheromone of ant passing through the node is updated.
- (5) The termination condition: the maximum number of iterations is reached, the iteration is stopped, and the optimal path is output. Otherwise, return to step (3) to continue to find the optimal path.

The flow chart of the improved ant colony algorithm (TGACO) is shown in Figure 6.

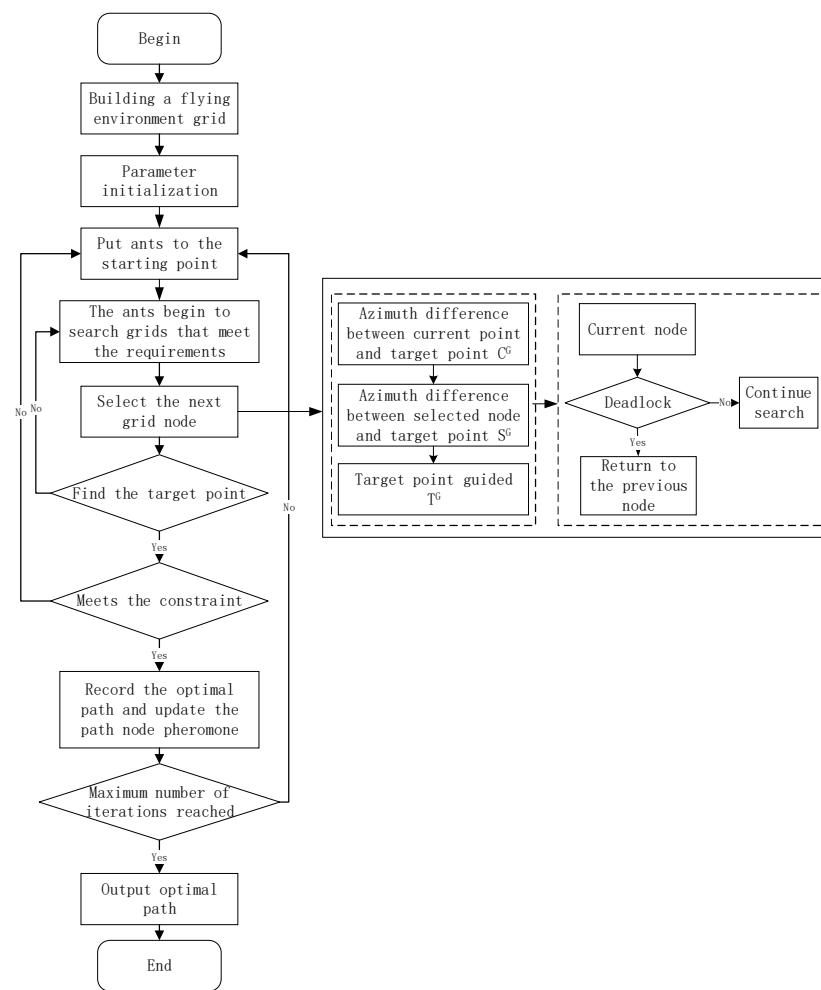


Figure 6. Flow chart of improved ant colony algorithm.

4. Simulation Experiments and Analysis

To verify the effectiveness and correctness of the improved ant colony algorithm (TGACO), the TGACO is simulated in different flight environments, and the advantages of the improved algorithm in efficiency, path quality, and other indicators are analyzed by comparing with other algorithms. The simulation environment is the Core (TM) i5 (2.40 GHz) Windows10 system.

4.1. Parameter Settings

The selection of different parameter values of the ant colony algorithm not only affects the time efficiency of operation, but also affects the quality of the solution. However, there is no perfect parameter value selection method in the existing research, so it is necessary to determine the parameter values of the ant colony algorithm through experiments and past experience [24]. In this paper, the parameter setting experiment is carried out in the $20 \times 20 \times 20$ grid environment, the single variable control method is adopted, and the best average value of 10 operation results is taken as the best parameter. Parameter intervals are $\alpha \in \{1, 2, 3, 4, 5\}$, $\beta \in \{1, 3, 5, 7, 9\}$, and $\rho \in \{0.2, 0.4, 0.5, 0.6, 0.8\}$. The default values are $\alpha = 1$, $\beta = 5$, and $\rho = 0.5$. The experimental results are shown in Table 1.

Table 1. Experimental results of main parameters.

Parameters	Parameter Settings and Experimental Results				
α	1	2	3	4	5
Mean path length	35.25	36.13	36.34	36.68	36.82
β	1	3	5	7	9
Mean path length	42.55	36.83	35.87	34.81	34.01
ρ	0.2	0.4	0.5	0.6	0.8
Mean path length	34.84	34.97	35.43	35.33	36.13

According to the experimental results, α is near 1, β is near 9, ρ is near 0.2, and the average path length is better. The weight coefficient of the heuristic function needs to be set according to the specific flight environment and experience. When there are few obstacles on the line between the starting point and the target point, target guidance can be taken as the main inspiration, so that the planned flight path is closer to the line between the two points. Therefore, the weight of target guidance can be set to a larger value. When there are many obstacles between the starting point and the target point, the weight of the target guidance should be appropriately reduced to avoid the algorithm falling into obstacles or local optimization. The weight experiment of the multi-objective function is shown in Table 2. The multi-objective function of distance and angle sets in this paper is significantly better than the single objective function of distance in terms of total angle and turning times, and there is a slight difference in distance. The weights of the multi-objective function are $\lambda_1 = 0.8$ and $\lambda_2 = 0.2$.

Table 2. Multi-objective function experiment.

Functions	Total Distance Mean	Total Angle Mean	Average Number of UAV Attitude Changes
Optimal path distance	33.81	376.5	12
Optimal path comprehensive	33.85	256.5	8

4.2. Algorithm Comparison Experiment

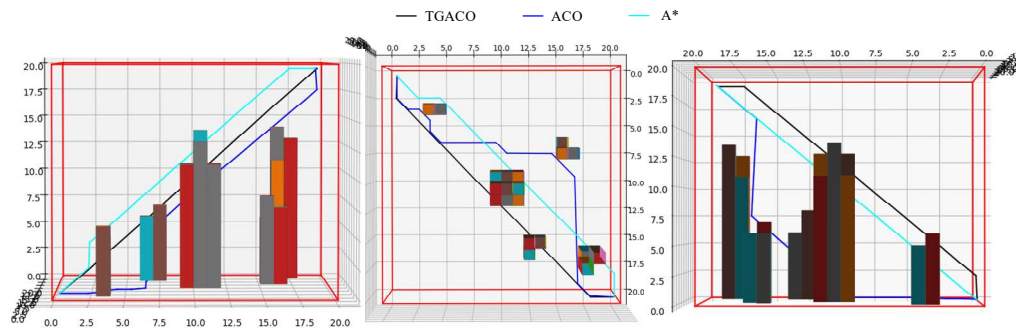
According to the parameter settings experiment, the optimal parameter values are selected as the parameters of the algorithm comparison experiments. The number of iterations of the ant colony algorithm (ACO) and improved algorithm (TGACO) is 50, the number of ants is 50, and the improved heuristic function weights are set according to the grid environment, starting point, and target point position. Since the starting point and the target point are in the diagonal position in the experiments, the target guidance weight is set to a larger value, and the heuristic function weights are $\mu_1 = 0.02$ and $\mu_2 = 0.98$.

(1) The $20 \times 20 \times 20$ Grid environment

In the $20 \times 20 \times 20$ obstacle grid environment, the improved ant colony algorithm (TGACO), ant colony algorithm (ACO), and A* algorithm are experimentally analyzed, and the four indexes of total path distance, total path angle, UAV attitude change times, and algorithm running time are compared, respectively. The experimental results are shown in Table 3. Compared with ACO, the TGACO has obvious advantages in four indexes, which are increased by 17.8%, 78.4%, 50%, and 95.3%, respectively. Compared with the A* algorithm, the TGACO algorithm improves the total angle, attitude change times, and running time by 28.9%, 33.3%, and 37.9%, respectively. The experimental results show that the proposed target guidance mechanism and anti-deadlock mechanism can effectively improve the speed and solution quality of the algorithm, and the multi-objective function can ensure that the UAV has fewer attitude changes and a smaller total turning angle. The planned paths of the three algorithms are shown in Figure 7.

Table 3. Environmental experiment results.

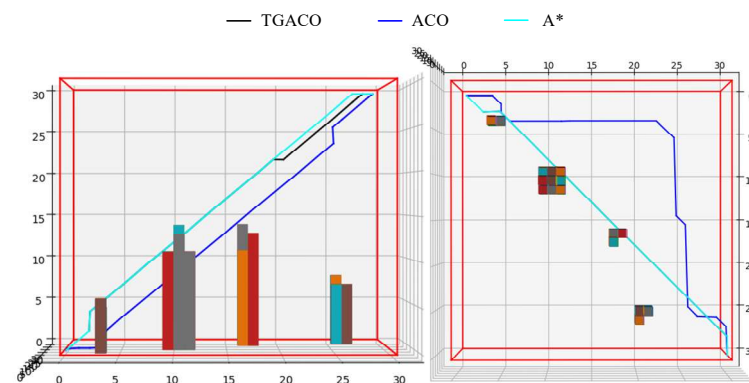
Algorithms	Total Distance	Total Angle	Attitude Change Times	Running Time(s)
TGACO	33.7	135	4	0.798
ACO	41.0	625	8	17.099
A*	33.7	190	6	1.285

**Figure 7.** Environmental planning path diagram.(2) The $30 \times 30 \times 30$ Grid environment

In the obstacle grid environment of $30 \times 30 \times 30$, the experimental analysis of three algorithms (TGACO, ACO, A*) is also carried out, and the four indexes in the above experiment are compared. The experimental results are shown in Table 4. Compared with the ACO, the TGACO has been greatly improved in terms of total distance, total angle, attitude change times, and algorithm running time, which are increased by 21.7%, 61.9%, 59.1%, and 99%, respectively. The advantages of the improved algorithm in algorithm running time are particularly obvious. Compared with the A* algorithm, although the TGACO does not have advantages in total distance, total angle, and attitude change times, it is 81.6% higher than the A* algorithm in running time. When the other three indexes are similar, the TGACO can better meet the requirements of UAV rapid path planning. The planned paths of the three algorithms are shown in Figure 8.

Table 4. Environmental experiment results.

Algorithms	Total Distance	Total Angle	Attitude Change Times	Running Time(s)
TGACO	50.8	280	9	2.262
ACO	64.9	735	22	224.262
A*	50.7	190	6	12.282

**Figure 8.** Environmental planning path diagram.(3) The $100 \times 100 \times 100$ Grid environment

Since path planning is an NP-hard problem, the running time of the algorithm increases exponentially by increasing the planning space. When the flight environment is too large,

ACO and A* algorithms cannot plan the flight path in a short time (10 min) and cannot meet the requirements of rapid path planning. The planning path of the improved algorithm (TGACO) in this environment is shown in Figure 9, and the experimental results are shown in Table 5.

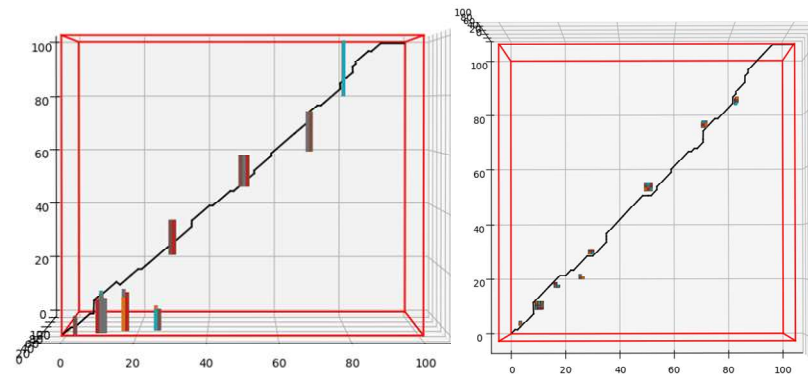


Figure 9. Environmental planning path diagram.

Table 5. Environmental experiment results.

Algorithms	Total Distance	Total Angle	Attitude Change Times	Running Time(s)
TGACO	183.2	3075	98	16.701

According to the results of experiments (1), (2), and (3), the improved algorithm TGACO in this paper has a certain degree of improvement in the total path distance, total path angle, UAV attitude change times, and running time, especially in the operation efficiency of the algorithm, which has obvious advantages. With the expansion of the UAV flight environment, the advantage of the improved algorithm in running time is more obvious.

5. Conclusions

To improve the accuracy and efficiency of the environment modeling, the flight environment grid map is established, and the 3D array is used to access the environment information, so that the UAV flight environment modeling is closer to the real situation and the environment information dimension is corresponding, thus effectively improving the reading efficiency of the flight environment information. To improve the insufficient path safety, a multi-objective function for UAV path planning is established. The function considers both the shortest path distance and the total angle of the path, to reduce the amplitude of variation and times of the UAV flight attitude change in the planned path and improve the safety of the planned path. The improved ant colony algorithm, proposed target guidance mechanism, and anti-deadlock mechanism effectively improved the global search efficiency and the quality of algorithm solution, adopted improved node pheromone update rules, improved the efficiency of the algorithm operation, and prevented the algorithm from falling into local optimization. Last, the effectiveness of the improved algorithm TGACO in this paper is verified through simulation experiments and algorithm comparison, and the improved algorithm is beneficial to fast path planning in complex flight environments. In the $30 \times 30 \times 30$ environment, compared with the ant colony algorithm (ACO), the improved algorithm (TGACO) in this paper increases the path length, the total turning angle, and the running time by 21.73%, 61.90%, and 98.99%, respectively.

The follow-up research work will focus on the adaptability of weights and influence factors, reduce the participation of human testing and experience values, and enable dynamic adjustment of each parameter to improve the adaptability of the ant colony algorithm to various application environments and meet different requirements. In the aspect of algorithm solution quality, the pheromone distribution is optimized to avoid the occurrence of local optimum. The time and space complexity of the algorithm is further

optimized, the overall process of path planning technology is improved by combining information such as UAV sensors, and it is analyzed and tested in a practical application. Finally, facing the future development trend of UAVs, the cooperative path planning of multi-UAV is further studied.

Author Contributions: H.Z. and Z.J. proposed the improved ant colony algorithm in this paper. Y.X. performed the simulation experiment and analyzed the experiment results. H.Z. and F.C. checked the result. Z.J. and Y.X. wrote the manuscript. W.L. and Y.L. provided writing advice for the manuscript. All authors have read and agreed to the published version of the manuscript.

Funding: This research received no external funding.

Institutional Review Board Statement: Not applicable.

Informed Consent Statement: Not applicable.

Data Availability Statement: The authors confirm that all data generated or analyzed during this study are included in this published article.

Acknowledgments: We thank the reviewers for helping us to improve this paper. We appreciate the relevant staff providing us with the help.

Conflicts of Interest: The authors declare no conflict of interest.

References

1. Zhang, D.; Li, R. Research on Swarms Cooperative Path Planning Method Based on Intelligent Optimization Algorithm. *Tactical Missile Technol.* **2020**, *103*, 17–29.
2. Wu, P.; Li, T.; Cao, G.; Song, G. UCAV path planning based on improved chaotic bee colony algorithm. *China Sci. Pap.* **2021**, *16*, 301–306.
3. Shi, H.; Tian, C.; Ren, Y.; Jia, F. Route Planning of Small Fixed-wing UAV Based on Sparse A* Algorithm. *Ordnance Ind. Autom.* **2021**, *40*, 14–18, 39.
4. Han, Y.; Li, S. UAV Path Planning Based on Improved Artificial Potential Field. *Systems Engineering and Electronics*. 2021. Available online: <https://kns.cnki.net/kcms/detail/11.2422.TN.20210531.1117.014.html> (accessed on 10 March 2022).
5. Wenbin, B. Route Planning Algorithm for Fixed-Wing UAV. Master's Thesis, Harbin Engineering University, Harbin, China, 2019.
6. Jia, G. Research on Three-Dimensional Path Planning of UAV Based on Genetic Algorithm and Sparse A* Algorithm. Master's Thesis, Nanjing University of Posts and Telecommunications, Nanjing, China, 2017.
7. Miao, C.; Chen, G.; Yan, C.; Wu, Y. Path planning optimization of indoor mobile robot based on adaptive ant colony algorithm. *Comput. Ind. Eng.* **2021**, *156*, 1–10. [CrossRef]
8. Gao, Y. UAV Task Planning Based on Intelligent Optimal Algorithms. Master's Thesis, Nanjing University of Posts and Telecommunications, Nanjing, China, 2019.
9. Junyi, Z. Research on Coordinated Attack Strategy of Multi-Loitering Ammunition Based on Intelligent Algorithm. Master's Thesis, North University of China, Taiyuan, China, 2020.
10. Qing, W.; Haiming, X.; Pin, L.Y.U.; Rui, J.; Dongdong, M. Research on path planning of multi-rotor UAV based on improved ant colony algorithm. *J. Hefei Univ. Technol. (Nat. Sci.)* **2021**, *44*, 1172–1178.
11. Gu, J.J.; Cao, Q.X. Path planning for mobile robot in a 2.5-dimensional grid-based map. *Industrial Robot. Int. J.* **2011**, *38*, 315–321.
12. Weinan, W. Research on Modeling and Method for Cooperative Combat Task Planning of Multiple Cruise Flight Missiles. Master's Thesis, Harbin Institute of Technology, Harbin, China, 2013.
13. Qiong, W.; Meiwan, L.; Weijian, R.; Tianren, W. Overview of Common Algorithms for UAV Path Planning. *J. Jilin Univ. (Inf. Sci. Ed.)* **2019**, *37*, 58–67.
14. Kaili, X.; Haitao, Y.; Haiping, X. Research Status of Intelligent Track Planning Algorithm. *J. Ordnance Equip. Eng.* **2020**, *41*, 8–13, 34.
15. Shahid, N.; Abrar, M.; Ajmal, U.; Masroor, R.; Amjad, S.; Jeelani, M. Path planning in unmanned aerial vehicles: An optimistic overview. *Int. J. Commun. Syst.* **2022**, *35*, e5090. [CrossRef]
16. Wenzhen, L.; Fukang, L.; Zongyan, C.; Jia, Y.; Xinkun, Y.; Ningning, Z. Mobile Robot Path Planning Using An improved Ant Colony Algorithm. *Modul. Mach. Tool Autom. Manuf. Tech.* **2021**, *15*, 49–52.
17. Liu, J.; Anavatti, S.; Garratt, M.; Abbass, H.A. Modified continuous Ant Colony Optimisation for multiple Unmanned Ground Vehicle path planning. *Expert Syst. Appl.* **2022**, *196*, 116605. [CrossRef]
18. Dai, X.; Long, S.; Zhang, Z.; Gong, D. Mobile Robot Path Planning Based on Ant Colony Algorithm with A* Heuristic Method. *Front. Neurorobot.* **2019**, *13*, 15. [CrossRef] [PubMed]
19. Tian, W.; Yang, Z. A Grid-Map-Oriented UAV Flight Path Planning Algorithm Based on ACO Algorithm. *Commun. Signal Processing Syst. Lect. Notes Electr. Eng.* **2020**, *516*, 1206–1216.

20. Zhao, H.; Nie, Z.; Zhou, F.; Lu, S. A Compound Path Planning Algorithm for Mobile Robots. In Proceedings of the 2021 IEEE International Conference on Power Electronics, Computer Applications (ICPECA), Shenyang, China, 22–24 January 2021.
21. Li, J.; Xiong, Y.; She, J. An improved ant colony optimization for path planning with multiple UAVs. In Proceedings of the 2021 IEEE International Conference on Mechatronics (ICM), Kashiwa, Japan, 7–9 March 2021.
22. Blum, C.; Dorigo, M. The hyper-cube framework for ant colony optimization. *IEEE Trans. Syst. Man Cybern. Part B* **2004**, *34*, 1161–1172. [[CrossRef](#)] [[PubMed](#)]
23. Xiangyang, D.; Limin, Z.; Wei, F.; Miao, T. Robot Path Planning Based on Bidirectional Aggregation Ant Colony Optimization. *J. Syst. Simul.* **2021**, *34*, 1101. Available online: <https://kns.cnki.net/kcms/detail/11.3092.v.20210420.1808.002.html> (accessed on 18 November 2021).
24. Fulong, Y.; Jianping, Z. Optimal path planning of mobile robot based on improved ant colony algorithm. *Mod. Manuf. Eng.* **2021**, *65*, 38–47.